25th ABCM International Congress of Mechanical Engineering
October 20-25, 2019, Uberlândia, MG, Brazil

COB-2019-0753
AN ANALYSIS OF ENERGY CONSUMPTION AND AVERAGE POWER IN A TWO-ARM VERTICAL PLANAR ROBOTIC MANIPULATOR FOR DIFFERENT TRAJECTORIES

Matheus Ungaretti Borges[1]
Fernando Augusto Araujo Pinto[2]
Eduardo José Lima II[1,2]
[1]Programa de Pós-Graduação em Engenharia Mecânica (PPGMEC), Universidade Federal de Minas Gerais (UFMG)
[2]Departamento de Engenharia Mecânica (DEMEC), Universidade Federal de Minas Gerais (UFMG)
Av. Pres. Antônio Carlos, 6627 - Pampulha, Belo Horizonte - MG, 31270-901
matheusungaretti@gmail.com
pinto.faa@gmail.com
eduardo@demec.ufmg.br

Abstract.
With the advent of 4.0 industry robotic systems are being widely applied on manufacturing processes in order to improve the comprehension in areas such as trajectory planning, collision tracking and time optimisation. By researching these themes, robotic systems can perform better their tasks executing movements with precision and avoiding moving obstacles, e.g. humans and other robotic manipulators. Nowadays, hundreds of robotic manipulators are being used together in industries. Thus, understanding their dynamic behaviour is essential to further integrate them. In this context, even a small amount of energy saved per manipulator makes the difference. Despite the relevance of this topic, there are only few papers regarding manipulator's energy. In this paper, a two-arm vertical planar robotic manipulator with two degrees-of-freedom is modelled to analyse a movement from one point to another and to evaluate the energy consumption and the average power. The maximum velocity and the maximum acceleration an arm can reach are the parameters used in this study. In conjunction with a set of arms properties (length, diameter, material density, weight and inertial momentum) it is calculated the energy spent and average power to execute a movement. In this study, the influence of these parameters on the energy and power is analysed. Thus, the comprehension of this system can be further used to improve the design and also to define the best set of parameters to execute a task.

Keywords: *Automation, Robotics, Robotic manipulator, Energy consumption*

1. INTRODUCTION

With the advent of electronics in the last decades, automation is becoming a wide and strong area to be studied (Borges and Lima, 2018) and the development of robotic manipulator technologies is rapidly growing in 4.0 industry era (Widodo *et al.*, 2019). Since robotic systems are generally complex, research is needed to improve known systems and develop new applications (Abu-Dakka *et al.*, 2017).

Nowadays, trajectory planning (Biagiotti and Melchiorri, 2008; Craig, 2009; Selvam *et al.*, 2019), collision tracking (Björkenstam *et al.*, 2013; Bajcsy *et al.*, 2018) and time optimisation (Sahar and Hollerbach, 1986; Abu-Dakka *et al.*, 2017) are consolidated and are still being studied. However, few are the papers regarding energy in robotics (Björkenstam *et al.*, 2013; Aziz *et al.*, 2019). Research on these themes leads to better robotic manipulators usage providing preciseness and robustness to industrial manufacturing processes. For example, Computer Numeric Control machine is able to achieve a micrometre precision in machining processes (Kussul *et al.*, 2002; Camara *et al.*, 2012), and robots are able to execute collision-free tasks avoiding obstacles, including humans (Bajcsy *et al.*, 2018).

To solve this energy issue, there are some possible approaches: to adjust the manipulator's design, and to constrain parameters, such as velocity and acceleration. A study of energy consumption and average power of a simple setup is proposed in this paper: a vertical planar robotic manipulator with two arms and two degrees-of-freedom, referred as 2-DOF manipulator. The manipulator's dynamics is simulated for several maximum velocity and maximum acceleration, aided by an algorithm implemented in Python. This setup using only two degrees of freedom simplifies the direct and inverse kinematics equations reducing the number of system variables for each configuration and, consequently, the computational cost. The influence of velocity and acceleration parameters on the energy spent and on the average power

is assessed and discussed by varying them on the simulation. If direct and inverse kinematics and dynamic models are known for cases with more degrees of freedom, the methodology of this study can be adapted to analyse them.

2. METHODOLOGY

To analyse the influence of the studied parameters, it is proposed the implementation of an algorithm in Python to calculate the energy spent and the average power of the 2-DOF manipulator. The manipulator movement from one position to another is described in the subsections 2.1 and 2.2. The implemented algorithm simulates the system dynamics and is run for distinct pairs of positions. The inputs for this algorithm are the initial position (X_0, Y_0), the final position (X_f, Y_f), the maximum velocity ($\dot{\theta}_{max}$) and the maximum acceleration ($\ddot{\theta}_{max}$) limiting both arms movement.

The robotic manipulator movement from one point to another can be described by using the joint-space system or the Cartesian-space system. The movement in joint-space system ensures a smooth movement and no singularities on the path (Craig, 2009). In addition, this system is generally used in the industry when the manipulator is not executing a specific task, e.g. moving between operation points. In this situation, there is no necessity to plan the path, since the main objective is positioning the manipulator to the next activity. Since the path is not tracked, there is no necessity of calculating intermediate points, leading to less operations reducing the simulation time.

2.1 Kinematics equations

Figure 1 illustrates the 2-DOF manipulator composed by two arms: the arm_1 is connected to the surface by the actuator $servo$ 1 and also connected to arm_2 by the actuator $servo$ 2, summing up two degrees of freedom. Both arms has limited range of motion, rotating from -180° to 180°. Each arm has a set of properties: length (L), diameter (d) and material's density (ρ). The weight (w) and angular momentum (I) are calculated using these properties. On the algorithm, the arms are instantiated with a given set of values, although it can be rendered adaptable to be executed with different arm's length, diameter and material's density.

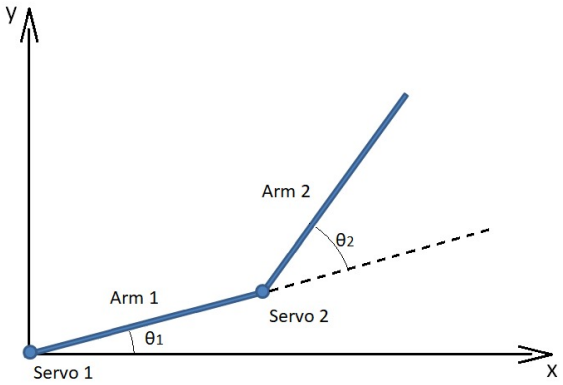

Figure 1. Vertical planar robotic manipulator scheme

Each point in the Cartesian system can be described on the joint space by the angles θ_1, between the surface and arm_1; and θ_2, between the arm_1 and the arm_2, as shown in Fig. 1. These angles are defined by the inverse kinematics as a function of its Cartesian coordinates, and its lengths L_1 and L_2 (Craig, 2009). The implemented algorithm calculates this pair of angles for the initial and final position, (θ_{1i}, θ_{2i}) and (θ_{1f}, θ_{2f}), respectively.

2.2 Trajectory planning

Once the kinematics equations are defined, the trajectory is planned to achieve the position and velocity profile illustrated on Fig. 2, (Lima II, 2005). The trajectory equations, Eq. (1) to Eq. (4), are written as a function of $\dot{\theta}_{max}$ and $\ddot{\theta}_{max}$.

As shown on Fig. 2, this movement can be characterised by three regions: region I, in which the arms accelerate steadily; region II, in which the arms move at constant velocity; and region III, in which the arms decelerate steadily. The rise time t_b is defined as the region I duration, which is the same for the region III; and the final time t_f is defined as the total movement duration (Lima II, 2005). It is also illustrated on Fig. 2 that the arms have the same values for t_b and for t_f. When synchronised, the arm movement soften the impacts on the system while operating.

In order to achieve the profiles shown on Fig. 2, the movement is mathematically modelled as stated by (Lima II, 2005). The final time, Eq. (1), the rise time, Eq. (2), and the restriction, Eq. (3), were used on the implemented algorithm to calculate the profile equation system, Eq. (4), according to the time movement.

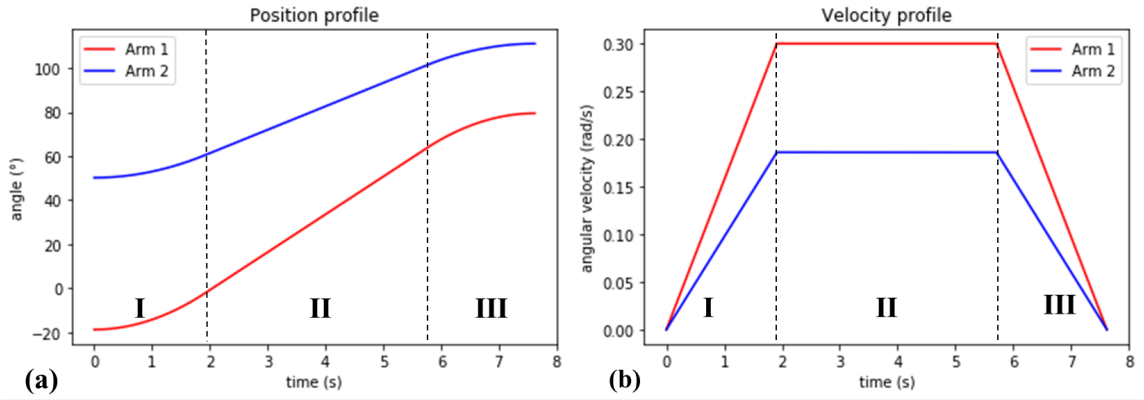

Figure 2. (a) Position profile and (b) Velocity profile generated for a generic movement

$$t_f = \frac{\ddot{\theta} t_b^2 + (\theta_f - \theta_0)}{\ddot{\theta} t_b} \tag{1}$$

$$t_b = \frac{\dot{\theta}_h}{\ddot{\theta}} \tag{2}$$

$$\ddot{\theta} \geq \frac{\dot{\theta}_h^2}{\theta_f - \theta_0} \tag{3}$$

$$\begin{cases} \theta_0 + \frac{1}{2}\ddot{\theta} t^2, & \text{if } t \leq t_b; \\ \theta_b + \dot{\theta}_h (t - t_b), & \text{if } t_b < t < (t_f - t_b); \\ \theta_f - \frac{1}{2}\ddot{\theta}(t_f - t)^2, & \text{if } t_f - t_b \leq t; \end{cases} \tag{4}$$

At this point, the movements are not synchronised yet and each arm has different t_b and t_f. Thus, it is necessary to synchronise the movement by updating the parameters $\dot{\theta}_h$, Eq. (5), and $\ddot{\theta}$, Eq. (6), for the fastest arm, since the slowest arm is the one limiting the combined movement. For example, if arm_2 movement is faster than arm_1 movement, then it should be updated. After applying these equations, the movement is now synchronous, i.e., the rise time and the final time are the same for both arms.

$$\dot{\theta}_{h2max} = \frac{\theta_{f2} - \theta_{i2}}{t_{f1} - t_{b1}} \tag{5}$$

$$\ddot{\theta}_{2max} = \frac{\theta_f - \theta_i}{t_{b1}} \tag{6}$$

2.3 Energy and power equations

After synchronising the movements, the energy spent, Eq. (7), by the 2-DOF manipulator to execute a movement is calculated as the sum of torque and velocity product for each instant, Eq. (8). The average power is defined as the ratio between energy spent and final time t_f, Eq. (9). The velocity and final time are defined on the subsection 2.2 . Sahar and Hollerbach (1986) define torque, Eq. (10), as a function of gravity and both arms' inertial momentum, mass, length, angular velocity, angular acceleration.

$$E = \int e dt \tag{7}$$

$$e = \tau \dot{\theta} \tag{8}$$

$$P = \frac{E}{t_f} \tag{9}$$

$$\tau_1 = f(g, I_1, I_2, m_1, m_2, l_1, l_2, \dot{\theta}_1, \ddot{\theta}_1, \dot{\theta}_2, \ddot{\theta}_2) \qquad \tau_2 = f(g, I_2, m_2, l_1, l_2, \dot{\theta}_1, \ddot{\theta}_1, \ddot{\theta}_2) \tag{10}$$

The implemented algorithm receives the inputs as describe at the beginning of section 2 and returns values of energy and power. Afterwards, the results are presented in graphs: energy versus velocity, energy versus acceleration, average power versus velocity and average power versus acceleration. Those outputs are analysed for different trajectories in the next section in order to better understand the influence of $\dot{\theta}$ and $\ddot{\theta}$ on the results.

3. RESULTS AND DISCUSSION

Table 1 shows the 2-DOF manipulator's arms standard properties as described on section 2. Those values correspond to an aluminium arm with 50 cm in length and 5 cm in diameter. The energy spent and average power are calculated for two movements on the Cartesian plane: $A = [(100, 0), (-50, 50)]$ and $B = [(-50, 0), (0, 100)]$, as shown in Fig. 3. The velocity and acceleration inputs are limited to $[\frac{\pi}{20}, \frac{3\pi}{20}]$ rad/s and $[\frac{\pi}{4}, \pi]$ rad/s^2, respectively. This limitation is done to better fit the algorithm inputs to the torque and energy equations (Sahar and Hollerbach, 1986).

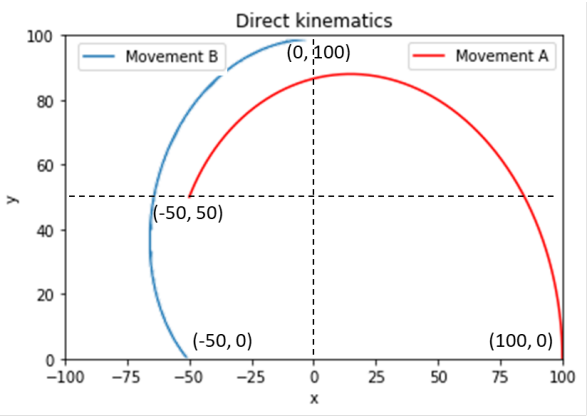

Figure 3. Direct kinematics for movements A and B

Table 1. Standard arm properties.

Arm	$L\ [m]$	$d\ [m]$	$\rho\ [kg/m^3]$	$w\ [kg]$	$I\ [Kg\ m^2]$
1	0.5000	0.0500	2700	0.5301	0.0443
2	0.5000	0.0500	2700	0.5301	0.0443

Figures 4(a) and 4(b) illustrate the velocity $\dot{\theta}_{max}$ and acceleration $\ddot{\theta}_{max}$ influence on the energy spent, respectively, for the movement A. It is noteworthy that the curves on Fig. 4(a) does not represent any correlation between the axes, i.e., the $\dot{\theta}_{max}$ influence on the energy spent is negligible. On the other hand, on Fig. 4(b) it is noticeable the correlation between the energy spent and the acceleration $\ddot{\theta}_{max}$. Set side by side, the curves on both figures emphasise the small influence velocity has on the energy spent.

Diverging from the behaviour shown previously, Fig. 5(a) and Fig. 5(b) illustrate the average power for the movement A. It is hypothesised the influence velocity $\dot{\theta}_{max}$ and acceleration $\ddot{\theta}_{max}$ have on average power due to the consistency shown on the different curves plotted on those graphs.

For movement B, the influence of parameters $\dot{\theta}_{max}$ and $\ddot{\theta}_{max}$ are illustrated in Fig. 6(a) and Fig. 6(b) for the energy spent, and in Fig. 7(a) and Fig. 7(b) for the average power. It is noteworthy that movement B behaves analogously to movement A.

By the comparison of Fig. 4 and Fig. 6, it is observed that both graphs are under the influence of acceleration and velocity parameters. The same influence pattern is observed when comparing Fig. 5 and Fig. 7 regarding average power. This congruence strengthen the previously mentioned hypothesis about the $\dot{\theta}$ and $\ddot{\theta}$ on the studied parameters.

Table 2 compiles energy data, Fig. 4 and Fig. 6, and power data, Fig. 5 and Fig. 7. These data are from the extremity points of the curve with the highest fixed acceleration ($max\ acc = 3.14\ rad/s^2$), represented in graphs with index (a);

and with the highest fixed velocity ($max\ vel = 0.47\ rad/s$), represent in graphs with index (b). For each movement, it is important to note that the far right values are equal, because they share the same values of velocity and acceleration used to calculate energy and power.

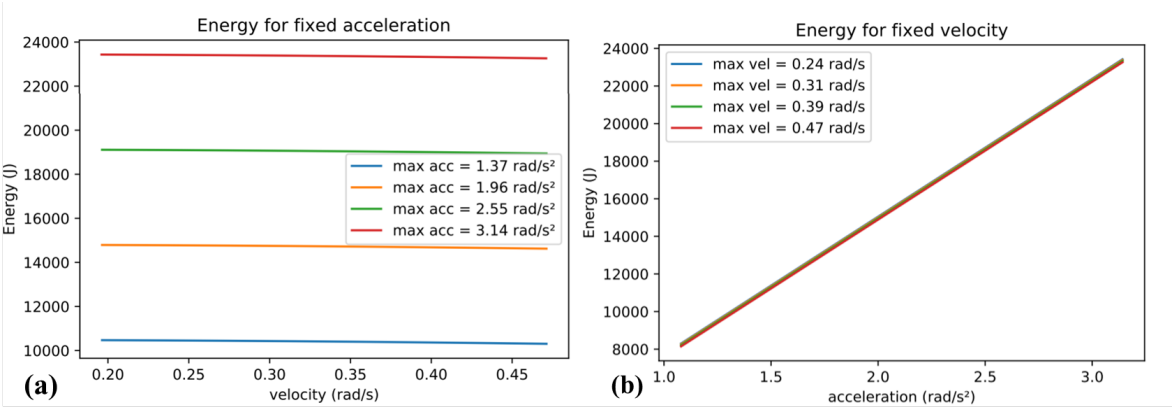

Figure 4. Movement A: (a) energy versus velocity; (b) energy versus acceleration

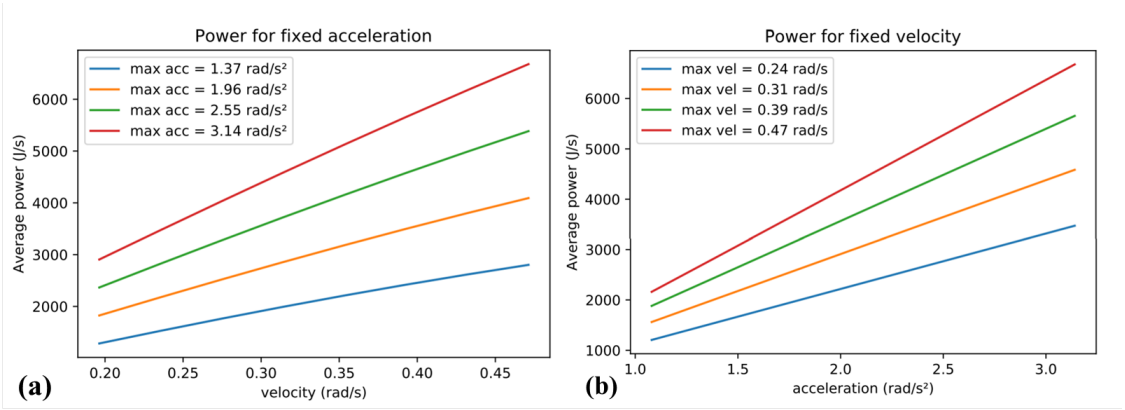

Figure 5. Movement A: (a) average power versus velocity; (b) average power versus acceleration

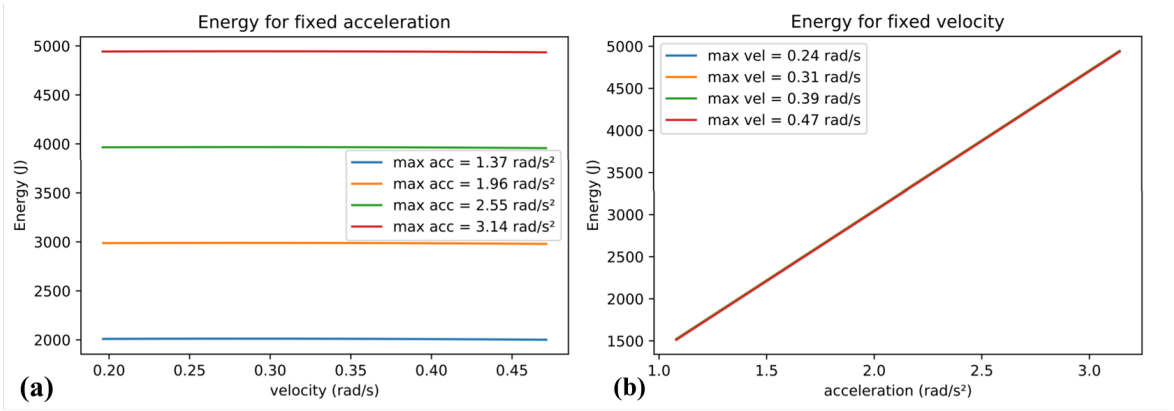

Figure 6. Movement B: (a) energy versus velocity; (b) energy versus acceleration

Furthermore, the general performance over Fig. 4 and Fig. 6 graphs is explained by the inverse relationship between the velocity $\dot{\theta}_{max}$ and the final time t_f (Craig, 2009); and the direct relationship between acceleration $\ddot{\theta}_{max}$ and torque (Sahar and Hollerbach, 1986). Increasing its $\dot{\theta}_{max}$, the 2-DOF manipulator is able to overcome the inertial momentum easily. In addition to the shortening of t_f, the energy spent to execute the movement A and B slightly decreases. In contrast, increasing the acceleration $\ddot{\theta}_{max}$ raises the torque required by the manipulator to execute the movement and, as a consequence, the energy spent increases significantly.

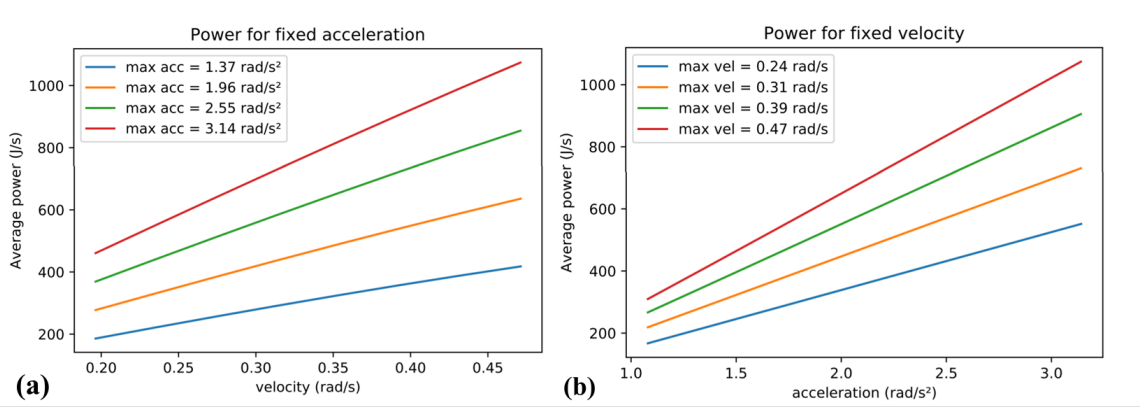

Figure 7. Movement B: (a) average power versus velocity; (b) average power versus acceleration

Table 2. Energy and power data.

	Movement A	Far left point	Far right point	Movement B	Far left point	Far right point
Energy $[J]$	Fig. 4(a)	23432	23261	Fig. 6(a)	4943.0	4934.7
	Fig. 4(b)	8145.9	23261	Fig. 6(b)	1512.1	4934.7
Power $[J/s]$	Fig. 5(a)	2906.2	6677.7	Fig. 7(a)	460.69	1074.0
	Fig. 5(b)	2160.8	6677.7	Fig. 7(b)	309.79	1074.0

Lastly, as previously mentioned, the average power is directly influenced by $\dot{\theta}_{max}$ and $\ddot{\theta}_{max}$. This is explained by the power definition as the ratio between energy spent and the final time t_f. The increase on $\ddot{\theta}_{max}$ raises the numerator energy spent by the manipulator and, consequently, the average power increases. Meanwhile, the increase on $\dot{\theta}_{max}$ decreases the denominator t_f and, hence, the average power increases as well.

4. CONCLUSION

On the technological context of 4.0 industry, hundreds of robotic manipulators are being applied on manufacturing processes. Although topics such as trajectory planning, collision tracking and time optimisation are consolidated, there is still a lack of understanding on the energy consumption of those systems.

This paper discuss the influence of the maximum velocity, $\dot{\theta}_{max}$, and the maximum acceleration, $\ddot{\theta}_{max}$, on the energy spent and average power on a vertical planar robotic manipulator with two arms and two degrees-of-freedom to execute a movement. After analysing the proposed movements, the correlation between the studied parameters, the energy spent and average power is verified. From the results of the studied setup, it is concluded that the velocity affects only the average power, whereas the acceleration also affects the energy spent. One can deduce that, for those movements, there is no extra energy cost to slow down a movement task, although this reduction implies greater final time and smaller average power.

This knowledge can be render adaptable by the project engineer to make better project decisions. From the experiment, it is observed that the average power provided by the manipulator can be set by several pairs of velocities and accelerations. Given the necessary power to execute a task, the project engineer can evaluate the best pair of parameters to match its power and time requirements, in previously mentioned tasks such as machining.

5. ACKNOWLEDGEMENTS

This study was financed in part by the Coordenação de Aperfeiçoamento de Pessoal de Nível Superior - Brasil (CAPES) - Finance Code 001.

6. REFERENCES

Abu-Dakka, F.J., Assad, I.F., Alkhdour, R.M. and Abderahim, M., 2017. "Statistical evaluation of an evolutionary algorithm for minimum time trajectory planning problem for industrial robots". *The International Journal of Advanced Manufacturing Technology*, Vol. 89, No. 1-4, pp. 389–406.

Aziz, M., Yahya, S., Almurib, H.A.F., Abakr, Y., Moghavvemi, M., Madibekov, Z., Elsayed, A. and Abdulrazic, M., 2019. "Torque minimized design of a light weight three dof planar manipulator". *IEEE Transactions on Industry Applications*.

Bajcsy, A., Herbert, S.L., Fridovich-Keil, D., Fisac, J.F., Deglurkar, S., Dragan, A.D. and Tomlin, C.J., 2018. "A scalable framework for real-time multi-robot, multi-human collision avoidance". *arXiv preprint arXiv:1811.05929*.

Biagiotti, L. and Melchiorri, C., 2008. *Trajectory planning for automatic machines and robots*. Springer Science & Business Media.

Björkenstam, S., Gleeson, D., Bohlin, R., Carlson, J.S. and Lennartson, B., 2013. "Energy efficient and collision free motion of industrial robots using optimal control". In *2013 IEEE international conference on automation science and engineering (CASE)*. IEEE, pp. 510–515.

Borges, M. and Lima, E., 2018. "Conversion methodologies from Signal Interpreted Petri Nets to Ladder Diagram and C language in Arduino". *International Journal of Mechanical Engineering Education*, Vol. 46, No. 4, pp. 302–314.

Camara, M., Rubio, J.C., Abrão, A. and Davim, J., 2012. "State of the art on micromilling of materials, a review". *Journal of Materials Science & Technology*, Vol. 28, No. 8, pp. 673–685.

Craig, J.J., 2009. *Introduction to robotics: mechanics and control*. Pearson Education India, 3rd edition.

Kussul, E., Baidyk, T., Ruiz-Huerta, L., Caballero-Ruiz, A., Velasco, G. and Kasatkina, L., 2002. "Development of micromachine tool prototypes for microfactories". *Journal of Micromechanics and Microengineering*, Vol. 12, No. 6, p. 795.

Lima II, E., 2005. "Soldagem robotizada com eletrodo revestido". *Programa de Pós-Graduação em Engenharia Mecânica da UFMG, Belo Horizonte, Minas Gerais, Brazil*.

Sahar, G. and Hollerbach, J.M., 1986. "Planning of minimum-time trajectories for robot arms". *The International journal of robotics research*, Vol. 5, No. 3, pp. 90–100.

Selvam, B., Natarajan, U., Balasubramonian, M. and Lakshmanaprabu, S., 2019. "Trajectory tracking control of two-link industrial robot manipulator based on c++". *International Journal of Rapid Manufacturing*, Vol. 8, No. 1-2, pp. 3–15.

Widodo, A., Muzakki, A. and Baskoro, F., 2019. "A 2-dof robot arm simulation for kinematics learning". In *2nd International Conference on Vocational Education and Training (ICOVET 2018)*. Atlantis Press.

7. RESPONSIBILITY NOTICE

The author(s) is (are) the only responsible for the printed material included in this paper.